Th17-cell plasticity in *Helicobacter hepaticus*–induced intestinal inflammation

PJ Morrison[1,5], D Bending[2,6], LA Fouser[3], JF Wright[3], B Stockinger[4], A Cooke[2] and MC Kullberg[1]

Bacterial-induced intestinal inflammation is crucially dependent on interleukin (IL)-23 and is associated with CD4$^+$ T helper type 1 (Th1) and Th17 responses. However, the relative contributions of these subsets during the induction and resolution of colitis in T-cell-sufficient hosts remain unknown. We report that *Helicobacter hepaticus*–induced typhlocolitis in specific pathogen-free IL-10$^{-/-}$ mice is associated with elevated frequencies and numbers of large intestinal interferon (IFN)-γ^+ and IFN-γ^+IL-17A$^+$ CD4$^+$ T cells. By assessing histone modifications and transcript levels in IFN-γ^+, IFN-γ^+IL-17A$^+$, and IL-17A$^+$ CD4$^+$ T cells isolated from the inflamed intestine, we show that Th17 cells are predisposed to upregulate the Th1 program and that they express IL-23R but not IL-12R. Using IL-17A fate-reporter mice, we further demonstrate that *H. hepaticus* infection gives rise to Th17 cells that extinguish IL-17A secretion and turn on IFN-γ within 10 days post bacterial inoculation. Together, our results suggest that bacterial-induced Th17 cells arising in disease-susceptible hosts contribute to intestinal pathology by switching phenotype, transitioning via an IFN-γ^+IL-17A$^+$ stage, to become IFN-γ^+ ex-Th17 cells.

INTRODUCTION

Inflammatory bowel disease, comprising Crohn's disease and ulcerative colitis, are chronic inflammatory disorders of the intestinal tract triggered by an inappropriate immune response to intestinal microflora.[1] Experimental models of the disease have revealed a crucial role for interleukin-23 (IL-23) in colitis pathogenesis,[2–5] and genome-wide association studies have further identified several single-nucleotide polymorphisms in the *IL23R* gene associated with either susceptibility or resistance to inflammatory bowel disease in humans.[6] IL-23 may contribute to the colitogenic response in several ways. Thus, this cytokine can inhibit the accumulation of intestinal Foxp3$^+$ Treg (regulatory T) cells, restrain iTreg-cell differentiation, act on IL-23R$^+$ T cells to inhibit IL-10 secretion by other CD4$^+$ T cells, and induce the production of T helper 17 (Th17)-type cytokines from innate lymphoid cells (reviewed in Maloy and Powrie[1] and Morrison *et al.*[7]). Another key function of IL-23 is to support the expansion and maintenance of Th17 cells, a CD4$^+$ subset that has evolved to protect the host from infectious assault at mucosal sites, and that is

characterized by its production of IL-17A, IL-17F, IL-21 and IL-22.[8,9] Much attention has recently focused on CD4$^+$ T cells co-expressing IL-17A and interferon (IFN)-γ, a lymphocyte population found in the inflamed intestine of both humans and mice,[10–12] as well as in the central nervous system of mice with experimental autoimmune encephalomyelitis (EAE).[13] The origin and role of IFN-γ/IL-17A double producers is not clear; however, IL-23R$^{-/-}$ CD45RB^{high} CD4$^+$ T cells fail to develop into IL-17A$^+$ IFN-γ^+ cells and do not trigger colitis in the T-cell transfer model,[12] showing that these lymphocytes develop through an IL-23-dependent pathway and may have an important role in disease pathogenesis.

We previously showed that inoculation with *Helicobacter hepaticus* (Hh) induces typhlocolitis in specific pathogen-free (SPF) IL-10$^{-/-}$ mice and in wild-type (WT) mice given anti-IL-10R monoclonal antibody (mAb).[5,14] Furthermore, treatment with anti-IFN-γ or anti-IL-12p40 mAb inhibits *Hh*-triggered colitis in IL-10$^{-/-}$ animals,[14] with IL-23 being the main driver of the inflammatory response triggered by this bacterium.[5] These observations demonstrate that both IL-23

and IFN-γ contribute to the development of T-cell-driven intestinal inflammation induced by *Hh*, strongly suggesting the involvement of Th1 and Th17 cells in the disease pathogenesis. However, the relative contributions of Th1 and Th17 cells to *Hh* colitis are so far unknown. Moreover, the plasticity of CD4$^+$ T cells at the site of inflammation in T-cell-sufficient hosts during the induction and resolution of bacterial-induced colitis is unclear. To address these issues, we characterized, at the single-cell level, the quality and quantity of lamina propria (LP) CD4$^+$ T cells induced by *Hh* challenge, considering the relationship between the T-cell response and the level of tissue inflammation.

Here we demonstrate that *Hh*-induced typhlocolitis in IL-10$^{-/-}$ mice correlates with elevated frequencies and numbers of intestinal LP CD4$^+$ T cells expressing IFN-γ or IFN-γ plus IL-17A. By analyzing histone modifications of CD4$^+$ subsets isolated from *Hh*-infected (*Hh*$^+$) IL-10$^{-/-}$ mice, we provide evidence that Th17 lymphocytes are predisposed to upregulate the Th1 program. Using an IL-17A fate-reporter system, we further demonstrate that, at peak pathology, a significant proportion of IFN-γ single-positive CD4$^+$ cells in the intestine are derived from lymphocytes that had previously expressed IL-17A. Together, our data suggest that bacterial-induced Th17 cells arising in disease-susceptible hosts contribute to pathology by switching phenotype, transitioning via an IFN-γ/IL-17A double-positive stage, to become IFN-γ$^+$ ex-Th17 cells.

RESULTS

CD4$^+$ T-cell responses in the large intestine of *Hh*-infected IL-10$^{-/-}$ mice

SPF IL-10$^{-/-}$ mice experimentally infected with *Hh* develop Th1/Th-associated typhlocolitis.[5,14] To begin to analyze the immune response at the site of inflammation in these hosts, we examined the cytokine secretion by tissue explants. Colon, but not small intestinal, explants from *Hh*$^+$ IL-10$^{-/-}$ mice secreted elevated amounts of IFN-γ and IL-17A compared with uninfected controls (**Figure 1a**), suggesting enhanced cytokine production at the site of *Hh* colonization and inflammation.[14,15] Colon explant supernatants also contained elevated levels of IL-1α, IL-6, and TNF-α but not IL-2, IL-4, or IL-5 (not shown). When large intestinal LP cells from 2-week *Hh*$^+$ IL-10$^{-/-}$ animals were examined, CD4$^+$ T cells were the major source of IFN-γ, IL-17A, IL-17F, and IL-22, with few non-CD4$^+$ cells producing these cytokines (**Figure 1b**).

The large intestine showed a significant change in LP cellularity during the course of *Hh* infection. Thus, total LP cell numbers peaked around 2–3 weeks post infection (pi) in both the colon and cecum, and thereafter declined at later time points analyzed (**Figure 2a**). Concurrent with the increased LP cellularity, the total number of CD4$^+$ T cells was elevated in both the colon and cecum between day 7 and day 45 pi (**Figure 2a**), a finding correlating with pathology in this model of T-cell-dependent colitis (**Figure 2b,c**). Luminal *Hh* concentrations increased between day 2 and day 4 pi, remained high through day 7 pi, and thereafter declined to reach a stable lower level colonization (**Figure 2d**).

These findings suggest that the bacterium goes through an early expansion phase in the intestine followed by the induction of a local anti-bacterial immune response resulting in inflammation; once bacterial burdens are controlled, the LP cellularity diminishes as the inflammation resolves (**Figure 2a–d**).

To examine the Th1/Th17 response during the course of infection, LP cells were isolated at different times post *Hh* inoculation and analyzed for their cytokine production. Colonic LP cells from uninfected, 2-, and 4-day *Hh*$^+$ IL-10$^{-/-}$ mice showed < 5% IFN-γ$^+$ or IL-17A$^+$ CD4$^+$ T cells (**Figure 2e**). By contrast, by day 7 pi there was a marked increase in the proportion of CD4$^+$ T cells staining positive for IFN-γ alone ($\sim$19%) or IL-17A alone ($\sim$9%), as well as the appearance of IFN-γ/IL-17A double-positive CD4$^+$ cells (**Figure 2e**). The proportion of IFN-γ single-positive lymphocytes remained high at $\sim$20% of the CD4$^+$ T cells during the following 2 weeks and thereafter declined (**Figure 2e**). A similar trend was seen for the IFN-γ$^+$IL-17A$^+$ population that peaked at $\sim$22% of CD4$^+$ cells by day 14–21 after *Hh* inoculation and thereafter declined (**Figure 2e**). By contrast, the proportion of IL-17A single-positive colonic CD4$^+$ T cells continued to increase during the course of infection, with the highest frequencies (24%) observed at day 91 pi (**Figure 2e**). The cecal LP CD4$^+$ T-cell response was comparable with that of the colon, with similar kinetics and percentages of IFN-γ$^+$, IL-17A$^+$, and IFN-γ$^+$IL-17A$^+$ cells in both tissues (**Figure 2g**, compare white and black bars). As for IFN-γ and IL-17A, the proportion of LP CD4$^+$ T cells expressing IL-17F or IL-22 was elevated from day 7 pi onwards (**Figure 2f,g**). The IL-17F$^+$ CD4$^+$ population showed a similar kinetics (although reduced in magnitude) to that of IL-17A$^+$ lymphocytes (**Figure 2g**). By contrast, IL-22$^+$ CD4$^+$ cells did not follow the same kinetics as the other Th17-cell populations, but correlated more closely with IFN-γ-expressing cells (**Figure 2g**), a finding similar to that reported for *in vitro*-cultured human CD4$^+$ T cells and for IL-22$^+$ effector memory CD4$^+$ cells that mainly co-produced IFN-γ rather than IL-17.[16]

Although the percentage of both IL-17A$^+$ and IL-17F$^+$ CD4$^+$ T cells increased during the course of infection, the absolute number of these cells was reduced at the later time points (**Figure 2h**). Similarly, the number of IFN-γ$^+$, IFN-γ$^+$IL-17A$^+$, and IL-22$^+$ CD4$^+$ T cells peaked by 2–3 weeks pi and thereafter declined (**Figure 2h**). At the time of maximal LP cellularity at 2–3 weeks pi, the IFN-γ single-positive and IFN-γ$^+$IL-17A$^+$ CD4$^+$ T cells were the two dominant populations observed (**Figure 2h**).

When colonic mRNA levels for Th1/Th17-polarizing cytokines were examined, IL-12p35 transcripts remained comparable with those of uninfected mice during the course of infection, whereas IL-12p40 mRNA was slightly elevated by day 7 pi, and thereafter reached levels significantly higher than those of uninfected controls by day 14, 21, and 45 pi (**Figure 2i**). TGF-β1 transcripts did not change significantly during the course of the experiment, but mRNA levels for IL-23p19 and IL-6 were significantly higher than those of uninfected controls by day 7 and days 7–14 pi, respectively (**Figure 2i**).
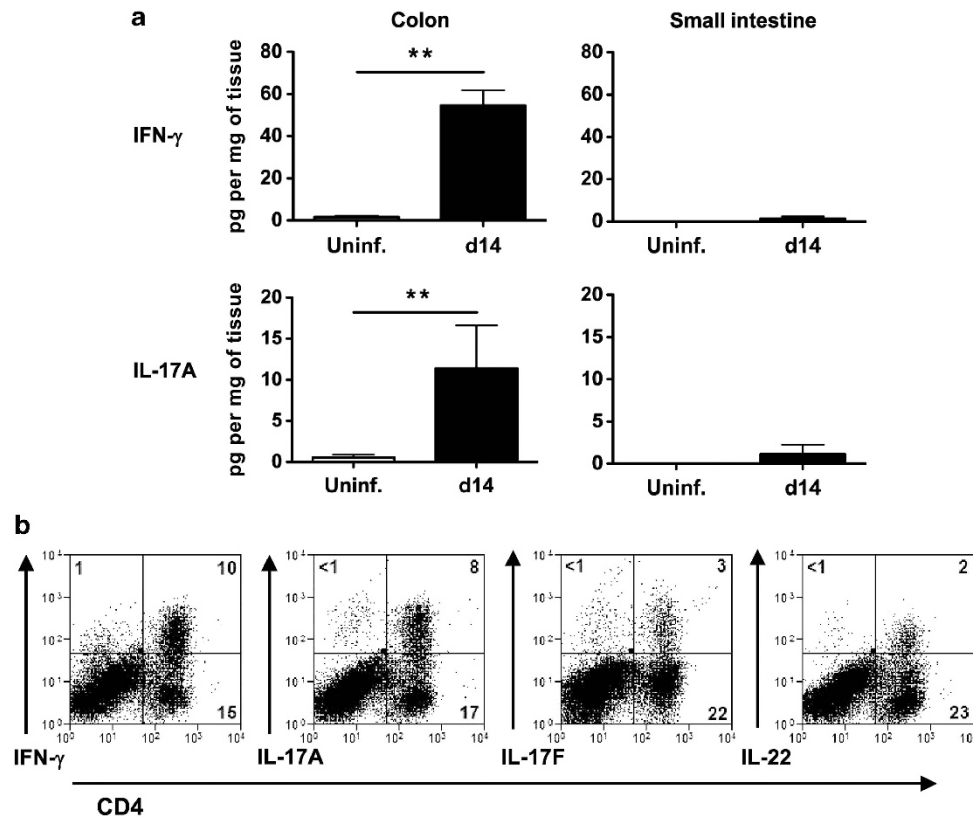
Figure 1 CD4^{+} T cells are the major source of T helper type 1 (Th1) and Th17 cytokines in the inflamed intestine of *Helicobacter hepaticus*-infected (*Hh*^{+}) interleukin (IL)-10[−/−] animals. IL-10^{−/−} mice were inoculated with *Hh*, and colon and small intestine collected 2 weeks later for explant cultures and lamina propria (LP) cell preparation. Uninfected (Uninf.) mice were included as controls. (**a**) Interferon (IFN)-γ and IL-17A in 24-h explant supernatants. Bars represent means ± s.e.m. of three individual mice per group. Data are representative of two independent experiments. (**b**) Colonic LP cells from 2-week *Hh*[+] IL-10^{−/−} mice were stimulated with phorbol myristate acetate/ionomycin and stained for CD4 and IFN-γ, IL-17A, IL-17F, or IL-22. Dot plots are representative of three independent experiments. CD4^{+} T cells were the major producers of Th1 and Th17 cytokines in the colon and cecum also at other time points examined (from day 2 to 91 pi; not shown).

Colonic IFN-γ^{+}IL-17A^{+} CD4^{+} T cells express T-bet and RORγt (RAR-related orphan receptor γt) and can produce IL-17F and IL-22

We next analyzed the LP CD4^{+} subsets for their expression of T-bet and RORγt. As expected, IFN-γ^{+} cells stained positive for T-bet and negative for RORγt, and IL-17A^{+} cells stained negative for T-bet and positive for RORγt (**Figure 3a–c**). Cells that failed to secrete IFN-γ and IL-17A were negative for both transcription factors. By contrast, IFN-γ^{+}IL-17A^{+} CD4^{+} cells expressed both T-bet and RORγt (**Figure 3a–c**), indicating similarities to both the Th1 and Th17 lineages.

When the expression levels of IL-17F and IL-22 were examined, IFN-γ/IL-17A double-negative and IFN-γ^{+} Th1 cells produced little or no IL-17F and IL-22, whereas both the IL-17A^{+} Th17 and the IFN-γ^{+}IL-17A^{+} cells contained significant proportions that produced IL-17F and/or IL-22, indicating a wide heterogeneity among IL-17A-secreting CD4^{+} cells (**Figure 3d**). The heterogeneity within the IL-17A^{+} population was further shown to change as a function of time after *Hh* inoculation. Thus, in the first couple of weeks post *Hh* challenge, a wider range of cytokine-secreting phenotypes were observed within the Th17 and IFN-γ^{+}IL-17A^{+}

populations, a heterogeneity that thereafter decreased as the inflammatory response diminished (**Figure 3e**).

Characterization of CD4^{+} subsets isolated from the LP of colitic mice

To further characterize the Th1, Th17, and IFN-γ^{+}IL-17A^{+} cells, a capture assay was used to sort live cytokine-secreting CD4^{+} subsets from the inflamed large intestine (**Figure 4a**). IFN-γ mRNA was highly expressed by *ex vivo* Th1 and IFN-γ^{+}IL-17A^{+} cells, whereas IL-17A and IL-22 transcripts were expressed primarily in the Th17 and IFN-γ[+]IL-17A^{+} populations (**Figure 4b**). IL-17F mRNA was mainly found in the Th17 lymphocytes, with no or low levels detected in Th1 and IFN-γ^{+}IL-17A^{+} CD4^{+} T cells (**Figure 4b**). These data are in agreement with results obtained by intracellular cytokine staining on LP cells where the Th17 population contained a higher proportion of IL-17F^{+} cells (and with brighter intensity of staining) compared with the IFN-γ[+]IL-17A^{+} population, whereas IL-22^{+} cells were distributed more equally between these two subsets (**Figure 3d**).

As predicted from intracellular cytokine staining data (**Figure 3b,c**), *ex vivo* Th1 and IFN-γ[+]IL-17A^{+}
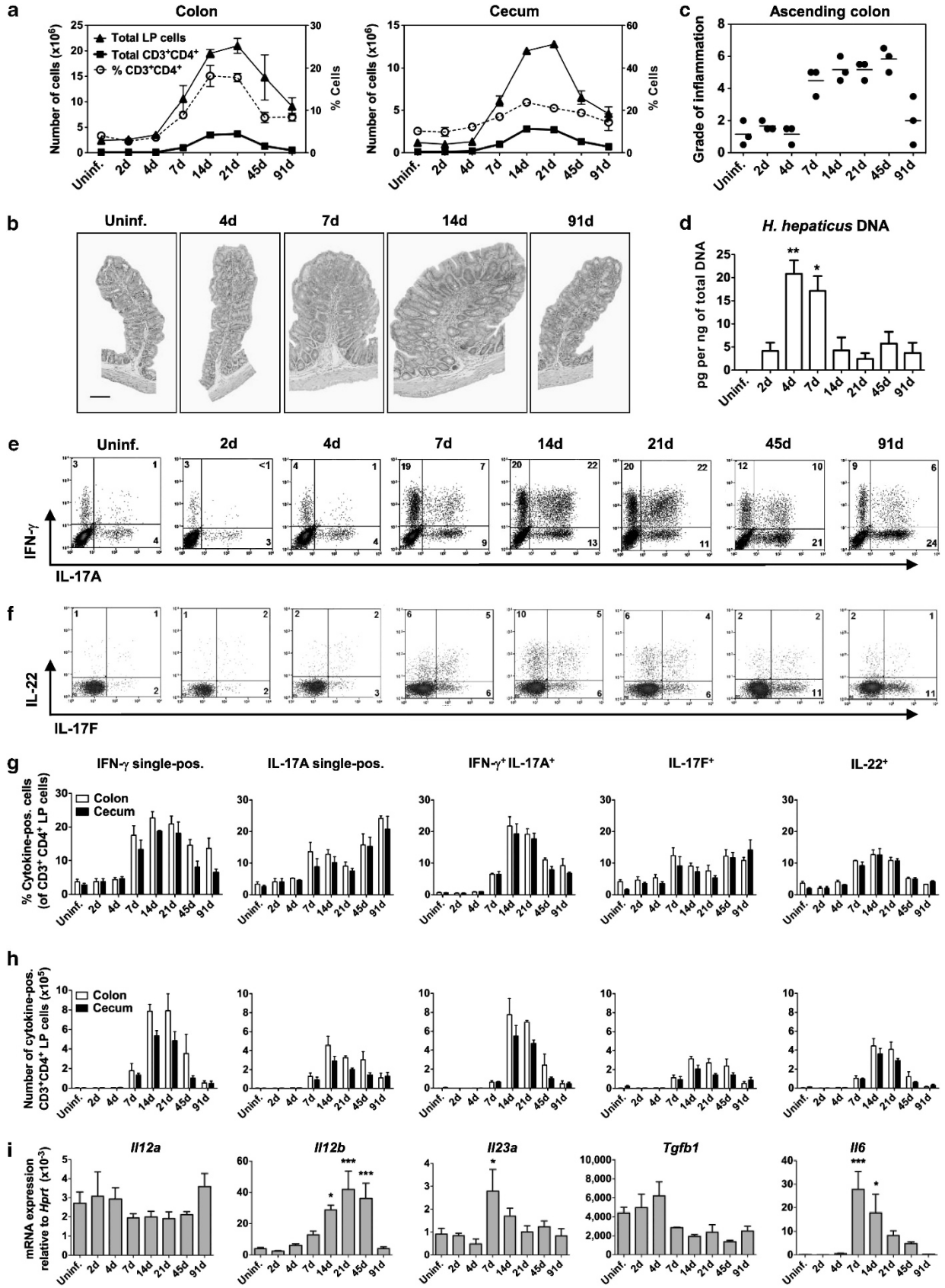
lymphocytes expressed significantly higher levels of T-bet mRNA compared with Th17 cells (**Figure 4c**). Furthermore, RORγt transcripts were significantly higher in Th17 cells than in the Th1 population, with IFN-γ$^+$IL-17A$^+$ cells expressing 3-4-fold more *Rorc* than Th1 cells (**Figure 4c**). Finally, AhR (aryl hydrocarbon receptor) mRNA was significantly upregulated in the Th17 population compared with the Th1 and IFN-γ$^+$IL-17A$^+$ populations (**Figure 4c**). Together, analysis of mRNA levels for cytokines and transcription factors indicate that IFN-γ$^+$IL-17A$^+$ CD4$^+$ cells induced by *Hh* inoculation show high similarities to Th1 cells but display a reduced Th17 program compared with traditional Th17 cells.

Ex vivo Th1, Th17, and IFN-γ$^+$IL-17A$^+$ LP subsets induce colitis

To examine the colitogenic capacity of the IFN-γ- and/or IL-17A-secreting *ex vivo* LP CD4$^+$ subsets, IFN-γ$^+$ Th1, IL-17A$^+$ Th17, and IFN-γ$^+$IL-17A$^+$ T cells were purified from the inflamed intestine of *Hh*$^+$ IL-10$^{-/-}$ mice and transferred to *Hh*$^+$ Rag$^{-/-}$ recipients. Rag$^{-/-}$ mice given *Hh* alone gained weight over the 4 weeks the animals were monitored, whereas recipients of Th1, Th17, or IFN-γ$^+$IL-17A$^+$ cells displayed a reduction in body weight over the same 4-week period (**Figure 5a**). Recipients of each of the three subsets developed colitis (**Figure 5b**). Moreover, phenotype analysis of the transferred subsets showed that Th17 and IFN-γ$^+$IL-17A$^+$ cells progressively switched towards a Th1-like phenotype. Thus, cells that were recovered 4 weeks post transfer from all the groups of Rag$^{-/-}$ recipients were largely IFN-γ$^+$, with the lymphocytes recovered from Th17 recipients also displaying some IFN-γ$^+$IL-17A$^+$ cells (**Figure 5c**).

Chromatin immunoprecipitation (ChIP) analysis of ex vivo LP CD4$^+$ subsets

We next performed ChIP analysis on the *ex vivo* CD4$^+$ subsets to assess H3K4me3 and H3K27me3 modifications at key genes involved in differentiation of Th1 (*Tbx21*/T-bet and *Ifng*) or Th17 (*Rorc* and *Il17a*) cells, as well as for the gene encoding the IL-12Rβ2 subunit (*Il12rb2*). *Ex vivo* Th17 cells exhibited permissive H3K4me3 modifications at *Rorc* and *Il17a* (**Figure 6a**, black bars). Moreover, the *Tbx21* locus of Th17 cells exhibited both H3K4me3 and H3K27me3 marks (**Figure 6a**, black bars), indicating that this gene may be poised for rapid activation. There was also no notable increase in H3K27me3 modifications at *Ifng* in these cells (**Figure 6a**,

black bars), suggesting that expression of IFN-γ may be rapidly upregulated without the need to remove repressive H3K27me3. Direct activation by IL-12 is unlikely, because *ex vivo* Th17 cells exhibited repressive H3K27me3 modifications at the *Il12rb2* locus (**Figure 6a**, black bars) and lacked IL-12Rβ2 transcripts (**Figure 6b**), suggesting that they lack a functional IL-12R. *Ex vivo* Th17 cells, however, expressed mRNA for *Il23r* and *Ifngr2* (**Figure 6b**).

IFN-γ$^+$IL-17A$^+$ CD4$^+$ lymphocytes displayed predominantly permissive H3K4me3 modifications at *Rorc*, *Tbx21*, *Il17a*, and *Ifng* (**Figure 6a**, gray bars). Moreover, the IFN-γ$^+$IL-17A$^+$ CD4$^+$ cells exhibited permissive H3K4me3 marks at *Il12rb2* (**Figure 6a**, gray bars), suggesting that these cells may be receptive to IL-12 signaling, a finding supported by the expression of both *Il12rb1* and *Il12rb2* mRNA in these cells (**Figure 6b**). IFN-γ$^+$IL-17A$^+$ cells also showed significantly reduced levels of *Il23r* and *Ifngr2* mRNA compared with Th17 cells (**Figure 6b**).

Ex vivo IFN-γ$^+$ Th1 lymphocytes exhibited permissive H3K4me3 modifications at *Tbx21*, *Ifng*, and *Il12rb2*, while displaying H3K27me3 marks at *Il17a* (**Figure 6a**, white bars). Although Th1 cells exhibited repressive H3K27me3 modifications at *Rorc*, this gene locus also showed signs of permissive H3K4me3 marks (**Figure 6a**, white bars). The presence of both marks at the *Rorc* locus could indicate that some of these IFN-γ$^+$ lymphocytes were once Th17 or IFN-γ$^+$IL-17A$^+$ cells but have repressed *Rorc* by adding H3K27me3 modifications during the process of phenotype switching.

Th17-cell phenotype switching in *Hh*$^+$ T-cell-sufficient mice

To formally examine whether IL-17A$^+$ CD4$^+$ lymphocytes convert to Th1-like cells in T cell-sufficient mice during *Hh*-induced colitis, we used a recently described IL-17A fate-reporter mouse in which cells that have turned on the IL-17A program will permanently express enhanced yellow fluorescent protein (eYFP).[17] CD45.1$^+$ WT mice were given busulfan followed by CD45.2$^+$ *Il17a*^{Cre}*R26R*^{eYFP} bone marrow cells to create microchimeric mice. Animals were subsequently inoculated with *Hh* and given anti-IL-10R mAb to induce colitis,[5] and their LP cells analyzed 2 weeks later. Donor-derived CD4$^+$ T cells constituted ∼20% of LP CD4$^+$ T cells (**Figure 7a**, left panel; 20.9 ± 7.5%, *n* = 4). When the phenotype of host vs. donor CD4$^+$ cells was analyzed, both populations displayed

---

Figure 2 CD4$^+$ T-cell responses in the large intestine of *Helicobacter hepaticus*-infected (*Hh*$^+$) interleukin (IL)-10$^{-/-}$ mice. IL-10$^{-/-}$ mice were inoculated with *Hh*, and colon and cecum collected 2, 4, 7, 14, 21, 45, and 91 days later. (**a**) Total lamina propria (LP) cell numbers (filled triangles), total CD3$^+$CD4$^+$ T-cell numbers (filled squares), and percentage of CD3$^+$CD4$^+$ T cells (open circles) in colon (left panel) and cecum (right panel). Each symbol represents the mean ± s.e.m. of 3 individual *Hh*$^+$ mice per time point and 14 uninfected (Uninf.) mice (2 per time point). (**b**) Histology of ascending colon from representative mice at 0, 4, 7, 14, and 91 days post infection. Hematoxylin and eosin stain. Bar = 100 μm. (**c**) Histology scores of ascending colon showing three individual mice per time point. (**d**) *Hh* colonization levels. Bars represent means ± s.e.m. of the mice in **a**. (**e–h**) LP cells stimulated with phorbol myristate acetate/ionomycin and stained for surface markers and intracellular cytokines. Dot plots are gated on colonic CD3$^+$CD4$^+$ T cells and show interferon (IFN)-γ and IL-17A (**e**) and IL-22 and IL-17F (**f**) and are representative of the mice in **a**. Frequencies (**g**) and total numbers (**h**) of LP CD3$^+$CD4$^+$ T cells from the colon (white bars) and cecum (black bars) that are IFN-γ single-positive, IL-17A single-positive, IFN-γ$^+$IL-17A$^+$, IL-17F$^+$, and IL-22$^+$. (**i**) Real-time reverse transcriptase–PCR analysis of colonic IL-12p35 (*Il12a*), IL-12p40 (*Il12b*), IL-23p19 (*Il23a*), transforming growth factor (TGF)-β1 (*Tgfb1*), and IL-6 (*Il6*) transcripts relative to HPRT (hypoxanthine-guanine phosphoribosyltransferase). Bars in **g–i** represent mean values ± s.e.m. of the mice in **a**. *$P < 0.05$, **$P < 0.01$, ***$P < 0.001$ compared with day 2 (for **d**) or uninfected controls (for **i**). Data shown are representative of three independent experiments performed (two using B6 IL-10$^{-/-}$ mice and one using B10 IL-10$^{-/-}$ mice).
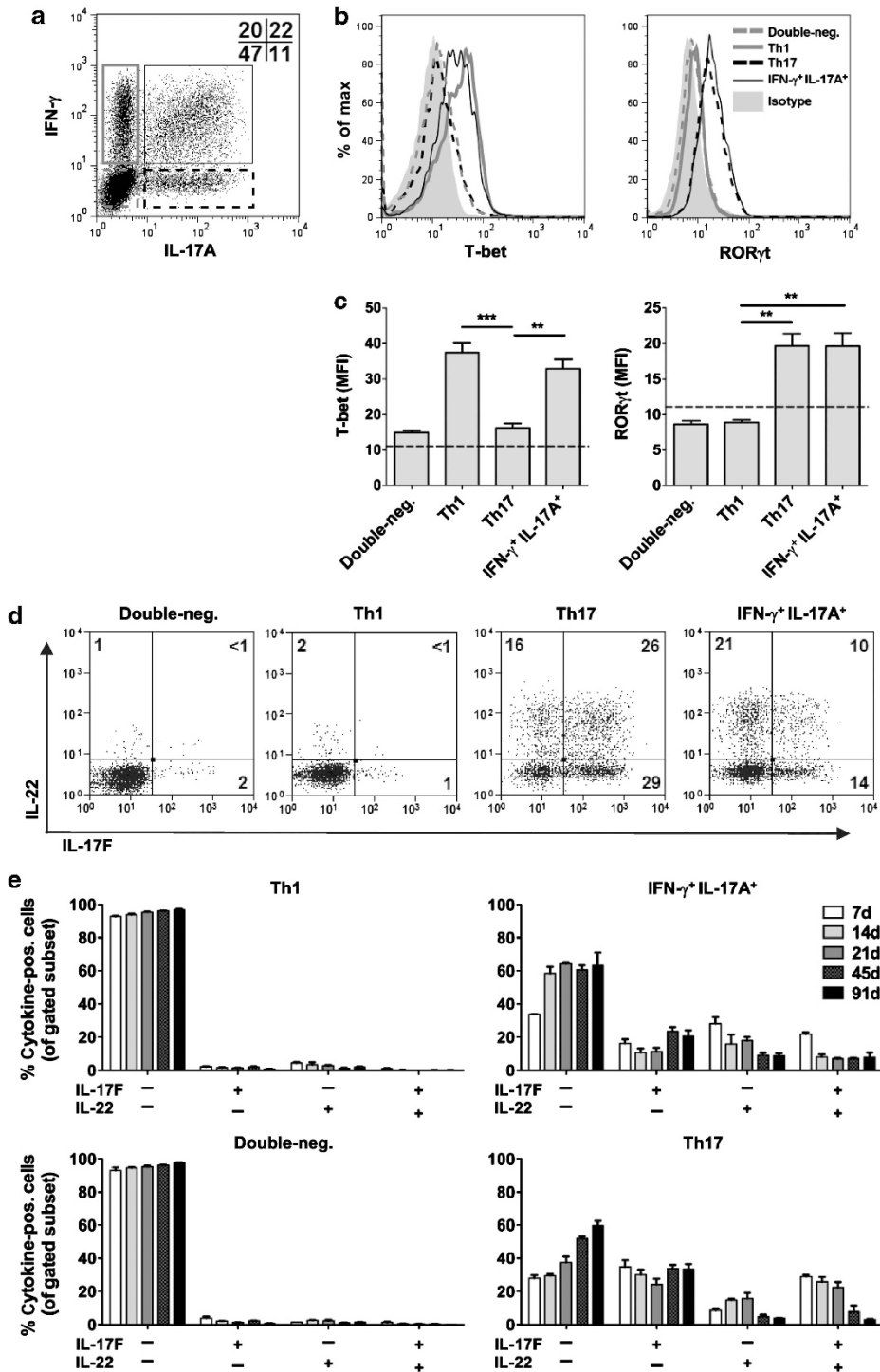
Figure 3 Interferon (IFN)-γ⁺IL-17A⁺ CD4⁺ T cells express T-bet and RORγt (RAR-related orphan receptor γt) and can produce interleukin (IL)-17F and IL-22. IL-10⁻ᐟ⁻ mice were inoculated with *Helicobacter hepaticus* (*Hh*), and colonic lamina propria (LP) cells were isolated (**a–d**) 2 weeks later or (**e**) 7, 14, 21, 45, and 91 days later and stimulated with phorbol myristate acetate/ionomycin followed by staining for flow cytometric analysis. (**a**) Dot plot gated on CD3⁺CD4⁺ T cells, illustrating the gating strategy for IFN-γ⁺ T helper type 1 (Th1; thick gray line), IL-17A⁺ Th17 (thick dashed black line), IFN-γ⁺IL-17A⁺ (thin black line), and IFN-γ/IL-17A double-negative (thick dashed gray line) cells. (**b, c**) Representative histograms in **b** with corresponding mean fluorescence intensity (MFI) graphed in **c** show T-bet and RORγt expression in the cytokine-secreting CD3⁺CD4⁺ subsets defined in **a**. Isotype control profiles (shaded) and corresponding MFI (dashed lines) in **b** and **c**, respectively, are shown for the total CD3⁺CD4⁺ population. Bars in **c** represent means ± s.e.m. of three individual mice. **P < 0.01, ***P < 0.001. (**d**) Dot plots show the expression of IL-22 and IL-17F in the Th1, Th17, IFN-γ⁺IL-17A⁺, and IFN-γ/IL-17A double-negative subsets defined in **a** at 2 weeks post infection (pi). (**e**) Quantification of the frequency of each of the 16 possible cytokine-secreting phenotypes of colonic LP CD4⁺ T cells based on IFN-γ, IL-17A, IL-17F, and IL-22 staining at 7, 14, 21, 45, and 91 days pi. Bars represent mean frequency ± s.e.m. of cytokine-positive cells from three individual mice per time point. Data are representative of at least two independent experiments.
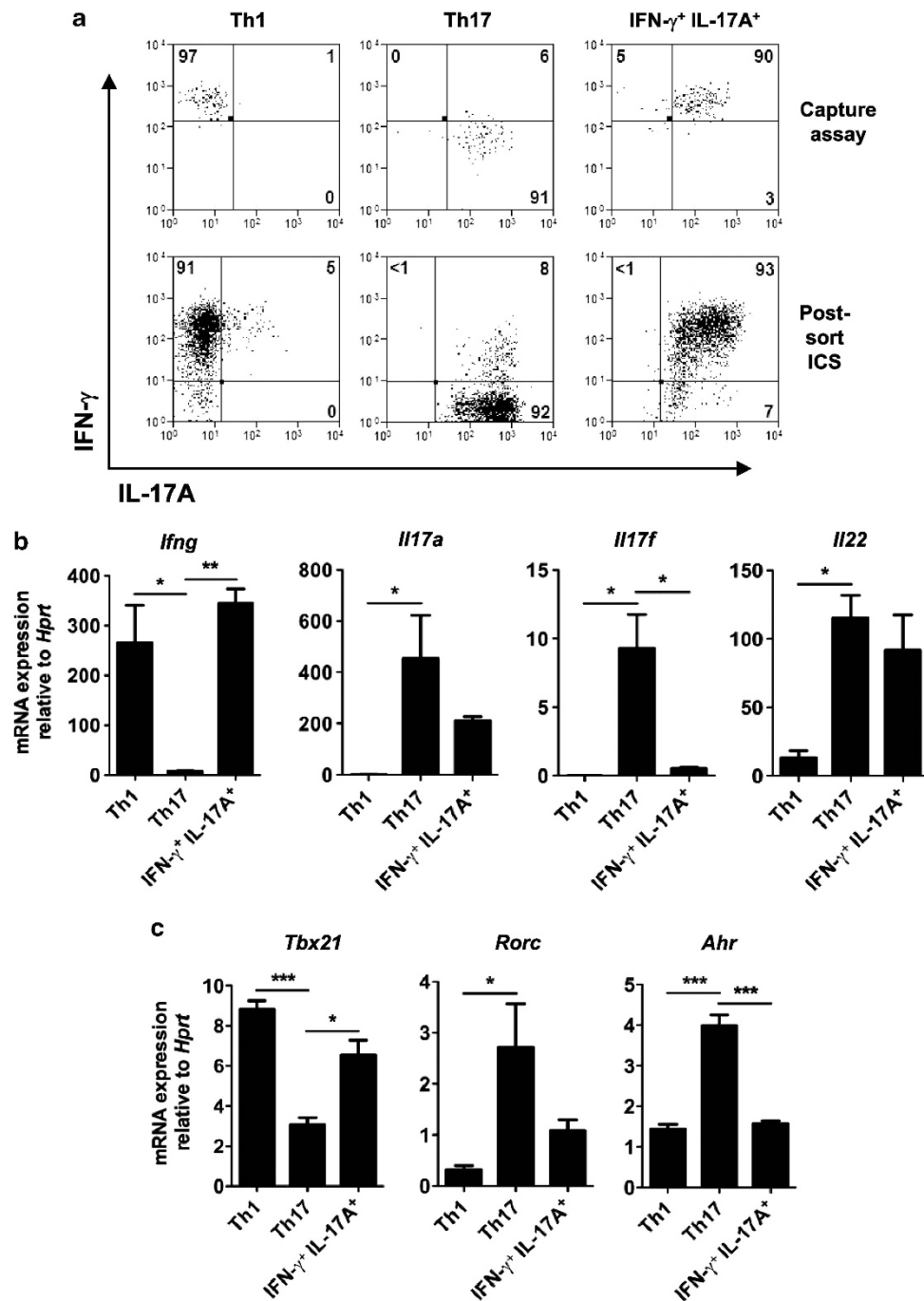
Figure 4 Cytokine and transcription factor expression by *ex vivo* lamina propria (LP) CD4$^+$ subsets. Large intestinal LP T helper type 1 (Th1), Th17, and interferon (IFN)-γ^+ IL-17A$^+$ CD4$^+$ subsets were purified from 2-week *Helicobacter hepaticus*-infected (*Hh$^+$*) interleukin (IL)-10$^{-/-}$ mice by cytokine-capture assay. Aliquots of sorted subsets were analyzed for post-sort purity by intracellular cytokine staining (ICS), and the rest of the cells were processed for analysis of cytokines and transcription factors. (**a**) Dot plots of sorted *ex vivo* CD4$^+$ subsets after capture-assay purification (top panels) and post-sort ICS analysis (bottom panels). (**b**, **c**) Cytokine in **b** and transcription factor in **c** mRNA expression levels in the sorted CD4$^+$ subsets. Bars represent mean mRNA levels relative to HPRT (hypoxanthine-guanine phosphoribosyltransferase) ± s.e.m. of three individual experiments, each consisting of cells pooled from 6–7 mice. *$P < 0.05$, **$P < 0.01$, ***$P < 0.001$.

similar proportions of IFN-γ^+, IL-17A$^+$, and IFN-γ^+IL-17A$^+$ cells (**Figure 7a**, right panels), ruling out any confounding effects due to the *Il17a^{Cre}R26R^{eYFP}* reporter. Within donor-derived lymphocytes, 38.3 ± 7.9% of CD4$^+$ T cells expressed eYFP in *Hh$^+$* anti-IL-10R-treated colitic mice,

indicative of these cells having turned on the IL-17A program (**Figure 7b**). By contrast, microchimeric mice given *Hh* alone showed <4% eYFP$^+$ donor CD4$^+$ T cells (**Figure 7b**), suggesting that the induction of IL-17A in the *Hh$^+$* anti-IL-10R group correlated with the development of inflammation.
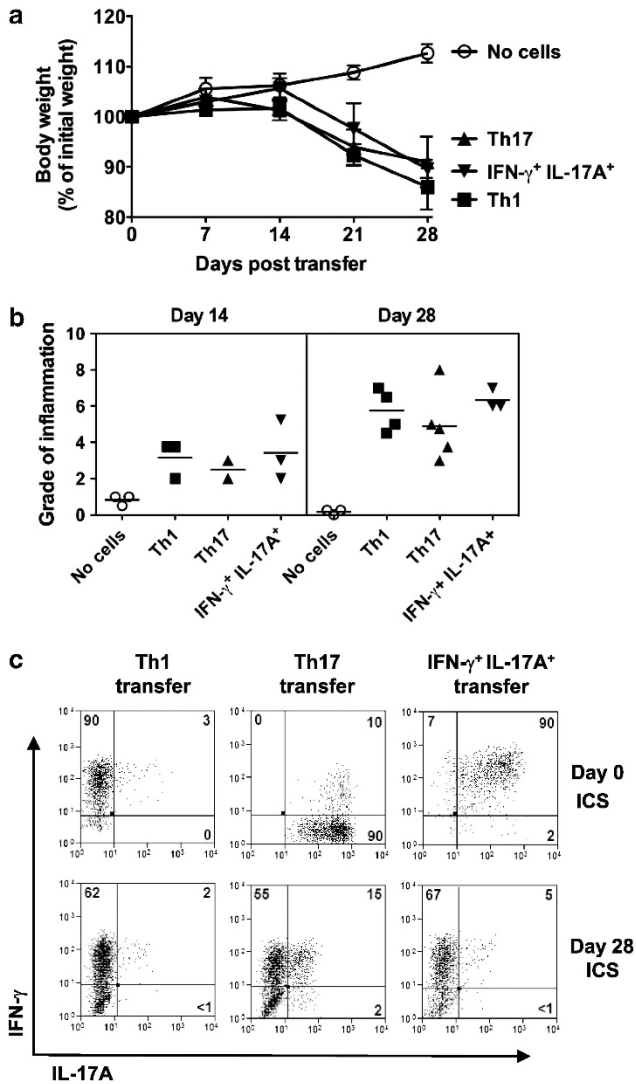
Figure 5 *Ex vivo* T helper type 1 (Th1), Th17, and interferon (IFN)-γ$^+$ IL-17A$^+$ CD4$^+$ cells induce weight loss and colitis after transfer to *Helicobacter hepaticus*-infected (Hh^+) Rag$^{-/-}$ mice. Large intestinal Th1, Th17, and IFN-γ$^+$ IL-17A$^+$ CD4$^+$ subsets were purified from 2-week Hh^+ interleukin (IL)-10$^{-/-}$ mice by cytokine-capture assay. 3×10^4 cells of each subset were transferred to groups of Rag$^{-/-}$ hosts that had been infected with Hh 2 days earlier. Hh^+ Rag$^{-/-}$ mice given no cells were included as controls. Body weights were measured weekly. At day 14 and day 28 post cell transfer, large intestinal lamina propria (LP) cells were isolated from the Hh^+ Rag$^{-/-}$ mice, stimulated with phorbol myristate acetate/ionomycin, labeled with a fixable live/dead dye, and stained for CD4, T-cell receptor β (TCRβ), IFN-γ, and IL-17A. (**a**) Mean body weight (relative to starting weight) ± s.e.m. of 4–7 mice per group and time point. (**b**) Histology scores of ascending colon of Hh^+ Rag$^{-/-}$ mice on day 14 and day 28 post cell transfer. Data are from 2–5 mice per group and time point and are pooled from four independent experiments. (**c**) Dot plots show IFN-γ and IL-17A staining of gated live CD4$^+$TCRβ$^+$ donor cells at time of transfer (day 0; top panels) and after recovery from the large intestinal LP of Hh^+ Rag$^{-/-}$ recipients 4 weeks later (day 28; bottom panels); dot plots are from one of four independent experiments. ICS, intracellular cytokine staining.

We next compared the cytokine-secretion phenotype of donor-derived eYFP$^-$ vs. eYFP$^+$ CD4$^+$ cells in the colitic mice. Among eYFP$^-$ CD4$^+$ T cells, IFN-γ single-positive lymphocytes constituted the major cytokine-producing population, comprising ~32% of the cells, whereas ~7% and ~8% secreted IL-17A or IFN-γ plus IL-17A, respectively (**Figure 7c**, left panels), a finding as previously reported likely due to these cells having just turned on IL-17A without reaching sufficient amounts of Cre recombinase to induce eYFP expression.[17] Among eYFP$^+$ CD4$^+$ lymphocytes, cells secreting IL-17A alone or IFN-γ plus IL-17A comprised ~18% and 41%, respectively (**Figure 7c**, right panels). Importantly, the eYFP$^+$ cells also contained a large population (~33%) expressing IFN-γ alone, without IL-17A expression (**Figure 7c**, right panels). These data demonstrate that CD4$^+$ T cells that have switched on the IL-17A program can subsequently extinguish their IL-17A production and become IFN-γ$^+$ ex-Th17 cells in Hh^+ colitic mice. When gating on total IFN-γ single-positive CD4$^+$ cells of donor origin, 31–49% of these cells expressed eYFP (**Figure 7d**), demonstrating that ex-Th17 cells represented up to half of the cells with a Th1-like phenotype at 2 weeks post Hh infection. When assessing the kinetics of phenotype conversion in Hh^+ anti-IL-10R-treated mice, at day 5 pi the frequency of eYFP$^+$ CD4$^+$ T cells was only marginally higher than that of mice given Hh alone (**Figure 7e**, left panel), and this small population predominantly expressed IL-17A alone with some increase in IFN-γ/IL-17A double producers observed (eYFP$^+$ CD4$^+$ T cells being IFN-γ$^+$ IL-17A$^+$: 16.5 ± 4.0% in the Hh^+ anti-IL-10R group ($n = 4$) vs. 9.0 ± 0.7% in the Hh alone group ($n = 3$)) (**Figure 7e**, right panel). As the frequency of eYFP$^+$ CD4$^+$ T cells increased by day 10 and day 14 pi (**Figure 7e**, left panel), the proportion of IL-17A single-producers deceased, whereas the percentage of both IFN-γ$^+$ IL-17A$^+$ and IFN-γ$^+$ ex-Th17 cells increased (**Figure 7e**, right panel). Together, these data indicate that IL-17A single-producing CD4$^+$ T cells progressively switch to an IFN-γ$^+$ ex-Th17 phenotype following bacterial inoculation and anti-IL-10R treatment.

DISCUSSION

Bacterial-induced intestinal inflammation is associated with Th1- and Th17-cell responses, but the relative contributions of these CD4$^+$ subsets to colitis pathogenesis in T-cell-sufficient hosts remain unknown. Here we show that intestinal inflammation triggered by Hh correlates with elevated frequencies and numbers of LP CD4$^+$ T cells expressing IFN-γ or IFN-γ plus IL-17A. We further demonstrate that IL-17A$^+$ lymphocytes arising after Hh inoculation extinguish their IL-17A secretion and transition to IFN-γ$^+$ ex-Th17 cells, together suggesting that Th17 cells contribute to pathology through phenotype switching.

Th17 cells have been implicated in multiple autoimmune and inflammatory disorders in both mouse and man,[18,19] and elevated levels of IL-17A, IL-17F, IL-21, and IL-22 have been found in the inflamed intestine in human inflammatory bowel disease as well as in experimental models of the disease.[7] Data from T-cell dependent colitis models have, however, failed to establish an essential role for T-cell-derived Th17 cytokines in intestinal pathology. Thus, IL-17A$^{-/-}$ CD45RB^{high} CD4$^+$ T cells, when transferred to Rag$^{-/-}$ recipients, induce intestinal
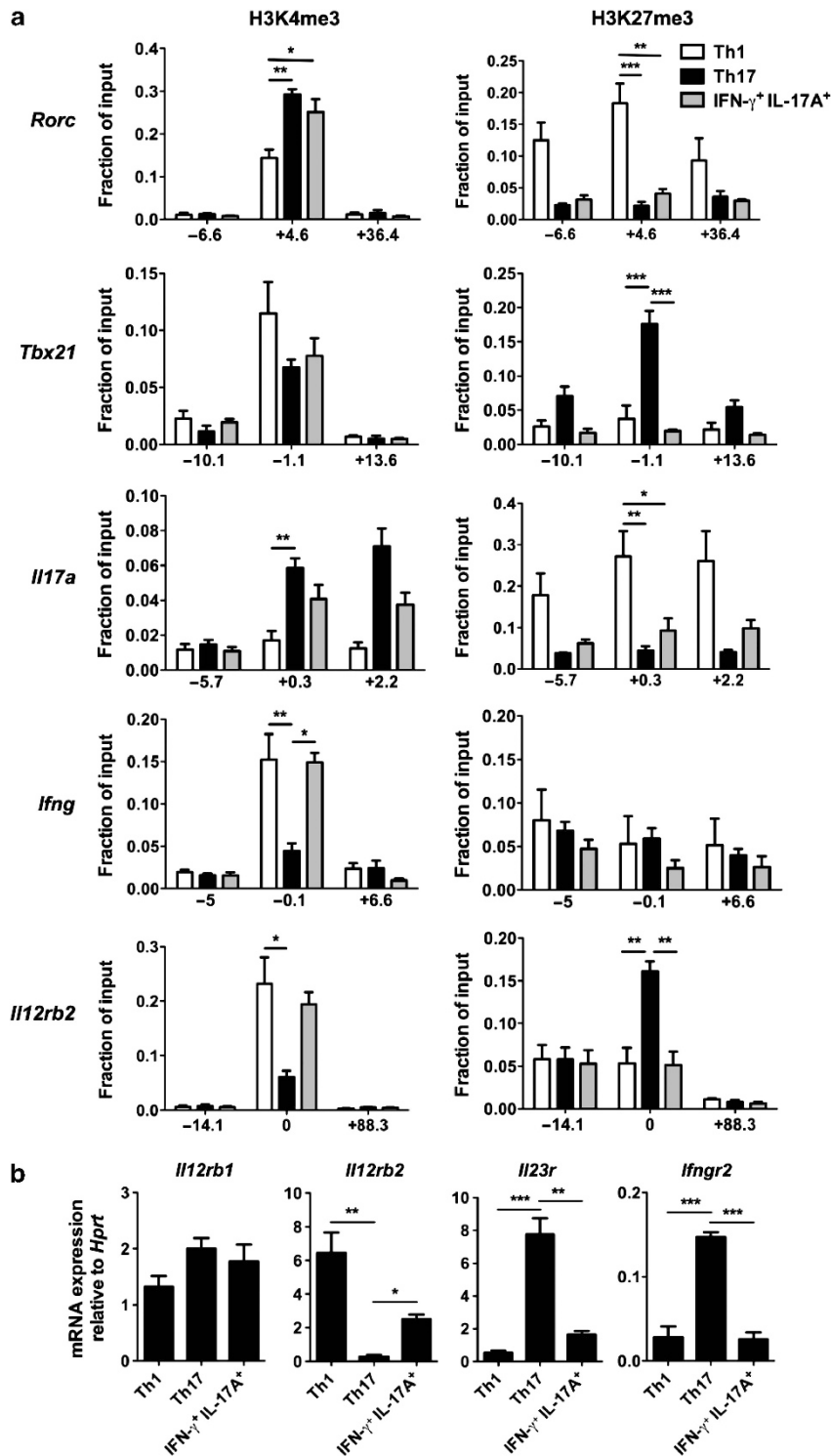
Figure 6 *Ex vivo* T helper type 17 (Th17) cells possess histone modifications that predispose them to upregulate the Th1 program. Large intestinal lamina propria Th1, Th17, and interferon (IFN)-γ$^+$ IL-17A$^+$ CD4$^+$ subsets were purified from 2-week *Helicobacter hepaticus*-infected (*Hh*$^+$) interleukin (IL)-10$^{-/-}$ mice and processed for chromatin immunoprecipitation analysis of histone modifications as well as real-time reverse transcriptase–PCR analysis of cytokine receptors. (**a**) Levels of immunoprecipitated DNA with H3K4me3 (left panels) or H3K27me3 modifications (right panels) normalized to input controls at the loci of the genes *Rorc*, *Tbx21*, *Il17a*, *Ifng*, and *Il12rb2* are shown for Th1 (white), Th17 (black) and IFN-γ$^+$ IL-17A$^+$ (gray) cells. Bars show mean levels ± s.e.m. of four individual experiments, each using cells pooled from 6–7 mice, except for *Il12rb2* for which three individual experiments were used. The x axis details the approximate location of the primers relative to 5′ untranslated region of the gene of interest in kb. (**b**) Cytokine receptor mRNA levels in *ex vivo* CD4$^+$ subsets. Bars represent mean mRNA expression levels relative to HPRT (hypoxanthine-guanine phosphoribosyltransferase) ± s.e.m. of three individual experiments, each consisting of cells pooled from 6–7 mice. *$P < 0.05$, **$P < 0.01$, ***$P < 0.001$.
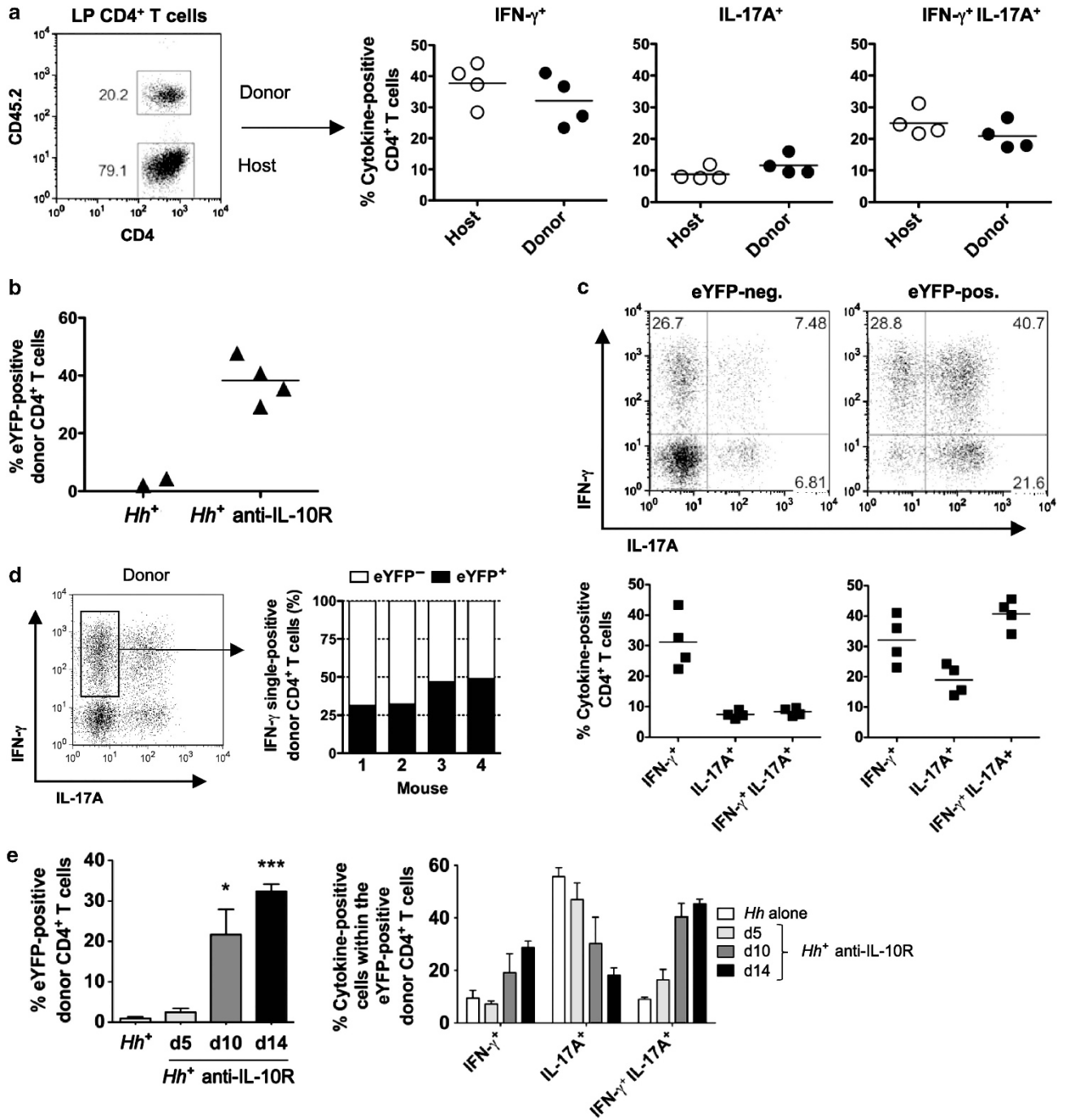
Figure 7 Phenotype switching of interleukin (IL)-17A[+] lymphocytes to T helper type 1 (Th1)-like ex-Th17 cells in *Helicobacter hepaticus*-infected (*Hh*[+]) T-cell-sufficient mice. Microchimeric *Il17a^{Cre}R26R^{eYFP}* animals were inoculated with *Hh* and given weekly injections of anti-IL-10R mAb to induce colitis. (**a**–**d**) Two weeks later or (**e**) 5, 10, and 14 days later, large intestinal lamina propria (LP) cells were isolated and stimulated with phorbol myristate acetate/ionomycin followed by labeling with a fixable live/dead dye and staining for flow cytometric analysis. (**a**) Left panel: Dot plot gated on live CD3^{+}CD4^{+} cells, showing proportion of donor-derived CD45.2^{+} *Il17a^{Cre}R26R^{eYFP}* CD4^{+} T cells in the LP. Three right panels: Comparison of the frequency of interferon (IFN)-γ^{+}, IL-17A^{+}, and IFN-γ^{+}IL-17A^{+} cells among CD4^{+} lymphocytes of host vs. donor origin. (**b**) Proportion of donor-derived CD45.2^{+} CD4^{+} T cells expressing eYFP^{+} (enhanced yellow fluorescent protein) in microchimeric mice given *Hh* alone vs. *Hh* plus anti-IL-10R mAb and analyzed at 2 weeks post infection (pi). (**c**) Top panels: Dot plots gated on eYFP^{-} vs. eYFP^{+} donor-derived CD45.2^{+} CD4^{+} T cells showing IFN-γ and IL-17A expression. Bottom panels: Graphs show the proportion of IFN-γ^{+}, IL-17A^{+}, and IFN-γ^{+}IL-17A^{+} cells within eYFP^{-} vs. eYFP^{+} donor-derived CD45.2^{+} CD4^{+} T-cell populations. Each symbol represents an individual mouse. (**d**) Left panel: Dot plot gated on donor-derived CD45.2^{+} CD4^{+} T cells showing IFN-γ and IL-17A expression. Right panel: Proportion of donor-derived IFN-γ single-positive CD4^{+} T cells within the eYFP^{-} vs. eYFP^{+} population. Each bar represents an individual mouse. Data in **a**–**d** are representative of two independent experiments performed. (**e**) Left panel: Proportion of donor-derived CD45.2^{+} CD4^{+} T cells expressing eYFP in microchimeric mice given *Hh* alone or *Hh* plus anti-IL-10R mAb and analyzed at 5, 10, and 14 days pi. Bars represent means ± s.e.m. of four individual *Hh*[+] anti-IL-10R-treated mice per time point and of three mice given *Hh* alone (one per time point). *P < 0.05, ***P < 0.001 compared with *Hh* alone. Right panel: Proportion of IFN-γ^{+}, IL-17A^{+}, and IFN-γ^{+}IL-17A^{+} cells within the eYFP^{+} donor-derived CD45.2^{+} CD4^{+} T-cell population. Bars represent means ± s.e.m. of the mice shown in the left panel.

inflammation indistinguishable from[20–22] or slightly enhanced[23] compared with that of WT T cells. Similarly, CD45RB^{high} CD4^{+} T cells isolated from IL-17F^{−/−} or IL-22^{−/−} animals induce colitis identical to that caused by WT T cells.[22] By contrast, CD4^{+} T cells deficient in signal transducer and activator of transcription factor 4 (STAT4), T-bet, STAT3, or RORγt have all been reported to be unable to induce colitis after transfer to T-cell-deficient hosts.[22,24–26] These findings argue that key regulators of Th1 and/or Th17 development, rather than cytokines produced by Th17 cells themselves, are needed to induce intestinal pathology. To our knowledge, it remains to be determined whether T-cell transfer colitis depends on a mixture of STAT4/T-bet-dependent Th1 and STAT3/RORγt-dependent Th17 lymphocytes, or if all four of these molecules are required in the same cell. In the latter scenario, STAT3/RORγt would be required for initial Th17-cell differentiation and STAT4/T-bet for subsequent conversion to an IFN-γ[+] IL-17A^{+} intermediate and subsequent IFN-γ[+] ex-Th17 cell,[7,17] one or both of which may contribute to pathology. It has been reported that in vitro-generated Th17 cells (<40% IL-17A^{+} cells at the time of transfer) are more potent than Th1 cells in inducing colitis in lymphopenic TCRβxδ^{−/−} (T-cell receptor βxδ^{−/−}) recipients, a finding the authors speculated was due to conversion to Th1 cells.[27] Data in support of the hypothesis that switching is essential for colitis pathogenesis come from Ahern et al.[12] who demonstrated that CD45RB^{high} CD4^{+} lymphocytes that fail to develop into IL-17A^{+} IFN-γ^{+} cells do not trigger intestinal inflammation in Rag^{−/−} recipients. Importantly, using microchimeric IL-17A fate-reporter mice, we demonstrate for the first time that phenotype conversion occurs in a colitic setting in non-lymphopenic hosts. Thus, we found that a large proportion of IFN-γ single-positive CD4^{+} lymphocytes in the inflamed intestine of T-cell-sufficient mice were once IL-17A^{+}, a finding analogous to that observed in the spinal cord of mice with EAE.[17] Hence, together, it is tempting to speculate that IL-17A^{+} cells are pathogenic in T-cell-sufficient hosts due to their ability to convert to IFN-γ^{+} cells.

Similar to that observed in inflamed tissue of Crohn's disease patients,[10,11] we found in the intestine of Hh^{+} IL-10^{−/−} colitic mice a population of IFN-γ^{+} IL-17A^{+} CD4^{+} cells. Moreover, the inflammatory response following bacterial inoculation correlated with elevated frequencies and numbers of both IFN-γ^{+} IL-17A^{+} and IFN-γ single-positive CD4^{+} cells. We further characterized IFN-γ^{+}, IFN-γ^{+} IL-17A^{+}, and IL-17A^{+} cells isolated from the inflamed intestine of Hh^{+} IL-10^{−/−} mice. Our findings demonstrate that ex vivo Th17 cells are predisposed to activate the Th1 program. Thus, IL-17A^{+} cells isolated from the inflamed intestine possessed both permissive and repressive marks at Tbx21, a finding in agreement with those previously reported for in vitro[28,29] and splenic ex vivo Th17 cells,[29] and could indicate the gene locus being in a poised state ready for rapid activation. Furthermore, the IFN-γ locus of ex vivo Th17 cells lacked repressive H3K27me3 marks, similar to that described for in vitro Th17 cells.[29,30] In contrast to their IL-17A single-

producing counterparts, ex vivo IL-17A^{+} IFN-γ^{+} cells—whose histone modifications have not been examined previously—displayed permissive marks at Il12rb2, suggesting the expression of a functional IL-12R, a finding supported by detectable mRNA levels for the two IL-12R subunits in these cells. To our knowledge, our findings represent the first example of ex vivo IFN-γ^{+}, IFN-γ^{+} IL-17A^{+}, and IL-17A^{+} CD4^{+} subsets being isolated from the same host for characterization of genes involved in Th-cell plasticity and effector choice, and support the concept that IL-17A^{+} T cells go through phenotype switching in Hh[+] colitic mice.

The cue(s) triggering switching of IL-17A^{+} cells during Hh-induced colitis remain unknown. Our experiments assessing the kinetics of phenotype conversion in Hh[+] anti-IL-10R-treated microchimeric IL-17A fate-reporter mice indicate a progressive switching with enhanced frequencies of eYFP[+] IFN-γ[+] IL-17A^{+} cells being detected as early as day 5 pi and ex-Th17 cells appearing between day 5 and day 10 pi. Moreover, from our temporal analysis in Hh^{+} IL-10^{−/−} mice, we found a large heterogeneity of CD4^{+} phenotypes in the intestine during the first few weeks after bacterial challenge that thereafter declined as the infection progressed, possibly as a result of the anti-bacterial immune response that controlled Hh burdens. Thus, the reduction in IFN-γ[+] IL-17A^{+} cells over time could be interpreted as a decline in switch rate due to diminished bacterial stimulation, something that eventually leads to resolution of inflammation. The signal(s) triggered by Hh that dictates phenotype switching is thus far unknown. Studies using in vitro-generated mouse and human Th17 cells have identified IL-12 as a potent inducer of conversion to a Th1-like state (reviewed in Morrison et al.[7]); however, IL-12 is unlikely to have a direct effect on Th17 cells in Hh[+] mice, as mRNA and ChIP analysis indicated that these cells lack a functional IL-12R. This finding is in agreement with previous observations demonstrating that ex vivo Th17 cells do not express IL-12Rβ2 and are unresponsive to IL-12.[29,31,32] Ex vivo Th17 cells can, however, be converted to a Th1-like phenotype following IFN-γ-induced upregulation of T-bet and acquisition of IL-12Rβ2.[29,32] Moreover, stimulation of AhR has been show to upregulate mRNA levels for both IL-12Rβ1 and IL-12Rβ2.[33] In this regard, Th17 cells isolated from the inflamed intestine of Hh[+] mice expressed elevated mRNA levels for both IFN-γR2 and AhR compared with IFN-γ[+] and IFN-γ[+] IL-17A^{+} cells. It has also become evident that IL-23 can influence Th-cell phenotype. Thus, IL-23 can induce IFN-γ production in in vitro-derived Th17 cells through a STAT4- and T-bet-dependent mechanism,[34] and recent data have demonstrated that this conversion involves IL-23-driven upregulation of T-bet also in vivo.[17] We hypothesize that phenotype switching in Hh[+] mice involves IL-23 acting on Th17 cells (**Figure 8**), as mRNA levels for IL-23p19 were elevated by 1 week post bacterial inoculation, and as ex vivo IL-17A^{+} cells isolated from the colitic intestine expressed both subunits of the IL-23R. This hypothesis is supported by studies in T-cell transfer colitis that demonstrated that T-cell intrinsic IL-23R signaling is necessary for CD45RB^{high} CD4^{+} cells to develop into IFN-γ/IL-17A

double producers.[12] Together, such a scenario links the essential role of IL-23 in *Hh* colitis pathogenesis[5] to IFN-γ+IL-17A+ and ex-Th17 cells that are increased in inflammation.

Taken together, the present study provides the first temporal analysis of intestinal CD4+ T-cell responses following infection with a colitis-inducing bacterium. Our data reveal a multi-faceted CD4+ T-cell response characterized by phenotype plasticity and conversion of IL-17A+ lymphocytes into IFN-γ+ ex-Th17 cells via an IFN-γ+IL-17A+ intermediate. This switching phenomenon may explain how Th17 cells contribute to intestinal inflammation and brings together previously published literature on the role of this CD4+ subset in colitis. More generally, combined with the description of ex-Th17 cells in EAE (but not in acute *Candida albicans* infection),[17] our findings in infection-induced colitis indicate that (i) IFN-γ single-positive CD4+ T cells found during chronic inflammation are not necessarily canonical Th1 cells, and (ii) ex-Th17 cells may contribute to disease pathogenesis in multiple inflammatory settings. In the case of colitis, there are several plausible means by which ex-Th17 (and IFN-γ+IL-17A+) cells could be involved in the disease process. First, these lymphocytes may contribute to pathology through their secretion of IFN-γ, a hypothesis in agreement with the documented role of this cytokine in colitis.[5,14,35–37] Second, ex-Th17 cells may secrete other factors that exacerbate the inflammatory response[17] (**Figure 8**). One such candidate is granulocyte macrophages colony-stimulating factor, a cytokine produced by Th17 cells and ex-Th17 cells[17] and shown to be pathogenic in EAE.[38,39] With neutralizing anti-IL-17A mAb failing to block T-cell transfer colitis in mice[22] and being ineffective in patients with Crohn's disease,[40] alternative strategies to target the Th17 response are needed. Continued characterization of Th1, ex-Th17, and IFN-γ+IL-17A+ cells and the factors they produce may help increase our understanding of the immunological processes active in the gastrointestinal tract of humans with inflammatory bowel disease and how to target these pathways for therapeutic approaches.

METHODS

Mice, infections, and mAb treatment. C57BL/6 (B6) IL-10−/−[41] (kindly provided by Dr A. O'Garra, NIMR), B6 CD45.1+ Rag2−/−, B6 CD45.1+ WT, and B6 CD45.2+ *Il17a^Cre R26R^eYFP* mice[17] were bred and maintained in an accredited SPF facility and experiments conducted in accordance with the UK Scientific Procedures Act (1986) under a Project License authorized by the UK Home Office Animal Procedures Committee and approved by the Ethical Review Committee at the Department of Biology, University of York, York, UK. Animals tested negative for antibodies to murine viruses, were free of *Helicobacter spp.* as assessed by PCR, and were >6-weeks old when used.

Microchimeric mice were generated by treating CD45.1+ WT mice with 400 μg busulfan intraperitoneally (Laboratories Pierre Fabre, Castres, France) followed 24 h later by 6 × 10^6 CD45.2+ *Il17a^Cre R26-R^eYFP* bone marrow cells intravenously. Microchimerism was examined 5 weeks later by flow cytometric analysis of blood, and mice were left for an additional week before use.
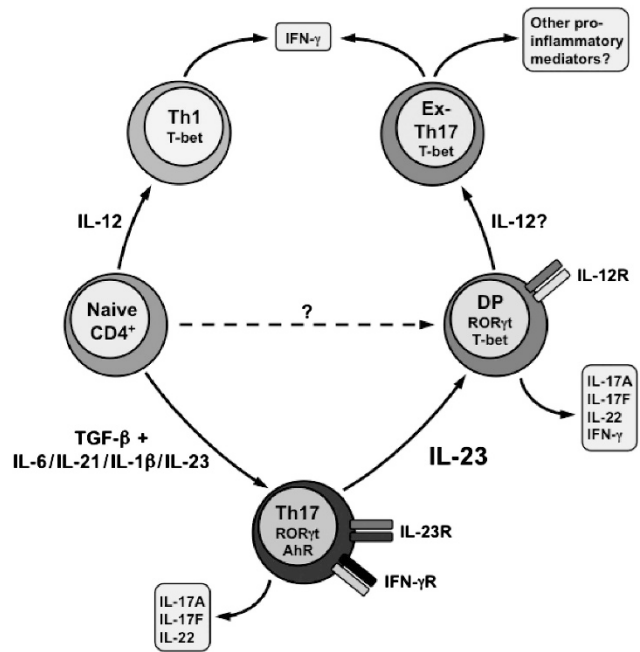

Figure 8 Model of CD4+ T-cell phenotype conversion during *Helicobacter hepaticus* (*Hh*)-induced colitis. Inoculation of disease-susceptible hosts with *Hh* causes CD4+ cells to differentiate into T helper type 1 (Th1) and Th17 lymphocytes. Interleukin (IL)-17A+ cells subsequently switch and transition via an interferon (IFN)-γ/IL-17A double-positive intermediate to become IFN-γ+ ex-Th17 cells. These ex-Th17 cells display similarities to Th1 cells but may also produce other pro-inflammatory mediators that contribute to the inflammatory response. AhR, aryl hydrocarbon receptor; RORγt, RAR-related orphan receptor γt; TGF, transforming growth factor.

Mice were inoculated intragastrically with 1.5 × 10^7 *Hh* NCI-Frederick isolate 1A,[42] isolated from the same mouse colony as isolate Hh-1[15] (American Type Culture Collection strain 51449). At different time points post *Hh* inoculation, intestines were collected for analysis. For some experiments, mice were treated intraperitoneally with 1 mg of mAb 1B1.3a (anti-IL-10R) on day 0 and day 7 of *Hh* infection, and tissues examined on day 5, 10, or 14 pi.

Intestinal explant cultures and cytokine determination. Tissue explants (~5 mm) of ascending colon and ileum were cultured overnight at 37 °C and 5% CO$_2$ in 0.5 ml complete medium (RPMI 1640 with 10% heat-inactivated fetal calf serum (FCS), 100 U ml−1 penicillin, 100 μg ml−1 streptomycin, 2 mM glutamine, 10 mM HEPES (4-(2-hydroxyethyl)-1-piperazineethanesulfonic acid), 1 mM sodium pyruvate, 0.1 mM nonessential amino acids, and 50 μM 2-ME) containing 50 μg ml−1 genticin, and supernatants stored at −80 °C until analysis of IFN-γ and IL-17A by enzyme-linked immunosorbent assay (Mabtech, Nacka Strand, Sweden).

Pathology. Tissues were fixed in buffered 10% formalin, and paraffin-embedded sections stained with hematoxylin and eosin (Mary Lyon Center at MRC Harwell, www.har.mrc.ac.uk). Samples were scored blindly from 0–3 for each of hyperplasia, LP infiltrating cells, and markers of severe inflammation (submucosal inflammation, crypt abscesses, ulcers). A total score was calculated by adding the individual scores.

LP cell isolation. Colons and ceca were cut into 3–5-mm pieces and incubated twice in RPMI 1640 containing 10 mM HEPES, 100 U ml−1 penicillin, 100 μg ml−1 streptomycin, 2 mM glutamine, 1% FCS, 1 mM dithiothreitol, and 5 mM EDTA for 20 min at 37 °C while shaking to release epithelial cells. Tissue pieces were then digested with Liberase

TL (0.3125 mg ml^{-1}; Roche, Burgess Hill, UK) and DNase I (0.125 U ml^{-1}; Sigma-Aldrich, Gillingham, UK) in RPMI 1640 containing 10 mM HEPES, 100 U ml^{-1} penicillin, 100 μg ml^{-1} streptomycin, 2 mM glutamine, and 1% FCS for 1 h at 37 °C while shaking. The resulting tissue suspension was passed through a 100-μm cell strainer, centrifuged, and resuspended in 40% Percoll and underlayed with 80% Percoll. After centrifugation at $600 \times g$ for 20 min at 10 °C, LP cells were recovered from the 40/80% interface and resuspended in complete medium.

Intracellular staining for cytokines and transcription factors. LP cells (5×10^6 per ml) were stimulated with 10 ng ml^{-1} of phorbol myristate acetate (PMA) and 1 μg ml^{-1} of ionomycin for 4 h at 37 °C with 10 μg ml^{-1} brefeldin A during the last 3 h. Thereafter, cells were resuspended in phosphate-buffered saline (PBS) containing anti-FcγRII/III mAb (2.4G2; 5 μg ml^{-1}; BD, Oxford, UK), stained at 4 °C with anti-CD3-PerCP (145-2C11; BD), anti-CD4-phycoerythrin (PE)-Cy7 (GK1.5; eBioscience, Hatfield, UK), and, in certain experiments, anti-CD45.2-PE (104; eBioscience), anti-TCRβ-PE (H57-597; BD), and a fixable Aqua Dead Cell stain (Invitrogen, Paisley, UK), washed with PBS, and fixed in 2% paraformaldehyde for 15 min. After a wash in PBS, cells were resuspended in permeabilization buffer (PBS containing Mg^{2+} and Ca^{2+}, 10 mM HEPES, 0.1% saponin, 1% FCS) with 10% normal mouse serum and 5 μg ml^{-1} anti-FcγRII/III, and incubated for 30 min at 4 °C. Thereafter, cells were stained for 30 min at 4 °C with combinations of mAb: anti-IL-17A-FITC (Mabtech), anti-IL-17A-PE (TC11-18H10; BD), anti-IFN-γ-eFluor450 (XMG1.2; eBioscience), anti-IL-17F-Alexa Fluor 647 (RK015-01; labeled in-house), anti-IL-22-Alexa Fluor 488 (IL-22-02; labeled in-house), washed with permeabilization buffer, and resuspended in PBS + 0.5% FCS. When staining for transcription factors, anti-RORγt-PE (AFKJS-9) and anti-T-bet-Alexa Fluor 647 (4B10) or appropriate isotype controls (all from eBioscience) were added from the start of the permeabilization step. Cell fluorescence was measured using a CyAn ADP flow cytometer (Beckman Coulter, High Wycombe, UK) and data analyzed using Summit (Beckman Coulter) or FlowJo software (Tree Star, Ashland, OR, USA). For **Figure 2a**, cell surface phenotypes were analyzed without previous stimulation by PMA/ionomycin.

Cytokine-capture assay. LP cells (3×10^7 per ml) from colons plus ceca pooled from 6–7 2-week Hh^+ IL-10$^{-/-}$ mice were stained with anti-CD4-FITC (RM4-5; BD), and CD4$^+$ cells sorted on a MoFlo (Beckman Coulter). Thereafter, live cytokine-secreting CD4$^+$ subsets were isolated by cytokine-capture assay. In brief, CD4$^+$ cells (10^7 per ml) were stimulated with 10 ng ml^{-1} of PMA and 1 μg ml^{-1} of ionomycin for 1.5 h at 37 °C, washed with PBS + 5% FCS (PBS/FCS), and labeled with pre-mixed IFN-γ and IL-17A capture reagents as recommended by the manufacturer (Miltenyi Biotec, Bisley, UK). Cells were then diluted to 4.5×10^4 per ml with RPMI + 5% FCS and incubated for 35 min at 37 °C, followed by labeling with anti-IL-17A-biotin (Miltenyi Biotec) and anti-IFN-γ-Alexa Fluor 647 (AN18; labeled in-house). Thereafter, cells were stained with anti-CD4-FITC, anti-CCR6-PE (140706; R&D Systems), and streptavidin-PE-Cy7 (eBioscience), and the four cytokine-secreting CD4$^+$ subsets (CCR6$^-$ IFN-γ$^+$ IL-17A$^-$ Th1, CCR6$^+$ IFN-γ$^-$ IL-17A$^+$ Th17, CCR6$^+$ IFN-γ$^+$ IL-17A$^+$, and CCR6$^-$ IFN-γ$^-$ IL-17A$^-$) were sorted on a MoFlo. To confirm post-sort purities, an aliquot of each subset was stimulated with 10 ng ml^{-1} of PMA, 1 μg ml^{-1} of ionomycin, and 10 μg ml^{-1} brefeldin A for 2.5 h at 37 °C, followed by intracellular cytokine staining for IFN-γ and IL-17A as described above but using different fluorochrome-labeled mAb than those used for the cytokine-capture assay.

Cell transfer to Rag$^{-/-}$ mice. Th1, Th17, and IFN-γ$^+$ IL-17A$^+$ CD4$^+$ cells isolated from the large intestine of 2-week Hh^+ IL-10$^{-/-}$ mice were transferred intravenously (3×10^4 per mouse) to 2-day Hh^+ Rag$^{-/-}$ recipients. Mice receiving no cells were included as controls. Two to four weeks after cell transfer, mice were killed, and intestinal tissues collected for histology and LP cell isolation.

Real-time reverse transcriptase–PCR. Ascending colon (3–5 mm) collected in RNAlater was homogenized in TRIzol, and total RNA was isolated by chloroform extraction followed by DNase treatment using the DNA-*free* kit (Applied Biosystems, Paisley, UK). Total RNA was isolated from *ex vivo* CD4$^+$ subsets using the RNeasy mini kit, including DNase treatment as recommended by the manufacturer (Qiagen, Crawley, UK). RNA from colonic tissue and CD4$^+$ subsets was reverse transcribed using SuperScript II and random hexamers. cDNA was amplified using SYBR green reagents and an ABI Prism 7300 Sequence Detection System (Applied Biosystems). Cytokine, cytokine receptor, and transcription factor expression levels for each individual sample (run in duplicates for tissue RNA and single or duplicate wells for subset RNA) were normalized to HPRT (hypoxanthine-guanine phosphoribosyltransferase) using ΔCt calculations. Primers pairs for murine *Il22*, *Il12rb1*, *Il12rb2*, *Il23r*, and *Ifngr2* were from Qiagen. Other specific primer pairs were: *Hprt*: 5′-GCGTCGTGATTAGCGATGATGAAC-3′, 5′-ATCTCCTTCATGA CATCTCGAGCAAGTC-3′; *Il12p40*: 5′-CATCAAGAGCAGTAGC AGTTCC-3′, 5′-GATACTTCTCATAGTCCCTTTGG-3′; *Il12p35*: 5′-AAATGAAGCTCTGCATCCTGC-3′, 5′-TCACCCTGTTGATGGT CACG-3′; *Il23p19*: 5′-CACATGCACCAGCGGGACAT-3′, 5′-CTTT GCAAGCAGAACTGGCTGTTG-3′; *Il6*: 5′-CTCTCTCTGCAAGA GACTTCC-3′, 5′-TGTGAAGTGGTATAGACAGGTCTG-3′; *Tgfb1*: 5′-ACCAAGGAGACGGAATACAG-3′, 5′-TCATGTCATGGATGG TGC-3′; *Ifng*: 5′-GGATGCATTCATGAGTATTGC-3′, 5′-GCTTCCT GAGGCTGGATTC-3′; *Il17a*: 5′-GCTCCAGAAGGCCCTCAG-3′, 5′-CTTTCCCTCCGCATTGACA-3′; *Il17f*: 5′-AGGGCATTTCTGT CCCACGTGAAT-3′, 5′-GCATTGATGCAGCCTGAGTGTCT-3′; and *Rorc*: 5′–ACCTCCACTGCCAGCTGTGTGCTGTC-3′, 5′-TCAT TTCTGCACTTCTGCATGTAGACTGTCCC-3′.

DNA was purified from cecal contents using QIAmp DNA Stool kit (Qiagen). *Hh* DNA was quantified as described[43,44] using real-time quantitative PCR for the *cdtB* gene, performed with an ABI Prism 7300 Sequence Detection System (Applied Biosystems). Standard curves were constructed using *Hh* DNA purified from bacterial cultures.

ChIP and DNA quantification. *Ex vivo* CD4$^+$ subsets were analyzed by ChIP as described.[29] In brief, cells were lysed, sonicated, and pre-cleared with normal rabbit serum, mouse immunoglobulin G1, and protein G agarose. An aliquot was taken as input control before samples were split and incubated overnight with antibodies to H3K4me3 (Abcam ab8580) or H3K27me3 (Abcam ab6002) (both from Abcam, Cambridge, UK). Thereafter, immune complexes were isolated with protein G agarose, eluted, and cross-links reversed before phenol/chloroform extraction of DNA followed by ethanol precipitation. DNA was then quantified by real-time PCR using Sensimix SYBR Lo-Rox (Qantace, London, UK) using primers designed for the promoter (arbitrarily defined as within the first kb upstream of the 5′ UTR of the gene of interest for *Tbx21*, *Ifng*, *Il17a*, and *Il12rb2* or +4585 bp for *Rorc*) plus upstream and downstream of the transcription start site; for sequences see Bending *et al.*[29] Data are presented as a fraction of input DNA.

Statistical analysis. Colon explant data were analyzed by Mann–Whitney U test. *Hh* colonization levels, mRNA expression, MFI data, ChIP data, and eYFP expression were analyzed by one-way analysis of variance. Differences were considered statistically significant with $P < 0.05$.

REFERENCES

1. Maloy, K.J. & Powrie, F. Intestinal homeostasis and its breakdown in inflammatory bowel disease. *Nature* **474**, 298–306 (2011).
2. Yen, D. *et al.* IL-23 is essential for T cell-mediated colitis and promotes inflammation via IL-17 and IL-6. *J. Clin. Invest.* **116**, 1310–1316 (2006).
3. Uhlig, H.H. *et al.* Differential activity of IL-12 and IL-23 in mucosal and systemic innate immune pathology. *Immunity* **25**, 309–318 (2006).
4. Hue, S. *et al.* Interleukin-23 drives innate and T cell-mediated intestinal inflammation. *J. Exp. Med.* **203**, 2473–2483 (2006).
5. Kullberg, M.C. *et al.* IL-23 plays a key role in *Helicobacter hepaticus*-induced T cell-dependent colitis. *J. Exp. Med.* **203**, 2485–2494 (2006).
6. Duerr, R.H. *et al.* A genome-wide association study identifies *IL23R* as an inflammatory bowel disease gene. *Science* **314**, 1461–1463 (2006).
7. Morrison, P.J., Ballantyne, S.J. & Kullberg, M.C. Interleukin-23 and T helper 17-type responses in intestinal inflammation: from cytokines to T-cell plasticity. *Immunology* **133**, 397–408 (2011).
8. Weaver, C.T., Hatton, R.D., Mangan, P.R. & Harrington, L.E. IL-17 family cytokines and the expanding diversity of effector T cell lineages. *Annu. Rev. Immunol.* **25**, 821–852 (2007).
9. McGeachy, M.J. & Cua, D.J. Th17 cell differentiation: the long and winding road. *Immunity* **28**, 445–453 (2008).
10. Annunziato, F. *et al.* Phenotypic and functional features of human Th17 cells. *J. Exp. Med.* **204**, 1849–1861 (2007).
11. Cosmi, L. *et al.* Human interleukin 17-producing cells originate from a CD161+CD4+ T cell precursor. *J. Exp. Med.* **205**, 1903–1916 (2008).
12. Ahern, P.P. *et al.* Interleukin-23 drives intestinal inflammation through direct activity on T cells. *Immunity* **33**, 279–288 (2010).
13. Suryani, S. & Sutton, I. An interferon-γ-producing Th1 subset is the major source of IL-17 in experimental autoimmune encephalitis. *J. Neuroimmunol.* **183**, 96–103 (2007).
14. Kullberg, M.C. *et al. Helicobacter hepaticus* triggers colitis in specific-pathogen-free interleukin-10 (IL-10)-deficient mice through an IL-12- and gamma interferon-dependent mechanism. *Infect. Immun.* **66**, 5157–5166 (1998).
15. Fox, J.G. *et al. Helicobacter hepaticus* sp. nov., a microaerophilic bacterium isolated from livers and intestinal mucosal scrapings from mice. *J. Clin. Microbiol.* **32**, 1238–1245 (1994).
16. Volpe, E. *et al.* Multiparametric analysis of cytokine-driven human Th17 differentiation reveals a differential regulation of IL-17 and IL-22 production. *Blood* **114**, 3610–3614 (2009).
17. Hirota, K. *et al.* Fate mapping of IL-17-producing T cells in inflammatory responses. *Nat. Immunol.* **12**, 255–263 (2011).
18. Korn, T., Oukka, M., Kuchroo, V. & Bettelli, E. Th17 cells: effector T cells with inflammatory properties. *Semin. Immunol.* **19**, 362–371 (2007).
19. Tesmer, L.A., Lundy, S.K., Sarkar, S. & Fox, D.A. Th17 cells in human disease. *Immunol. Rev.* **223**, 87–113 (2008).
20. Noguchi, D. *et al.* Blocking of IL-6 signaling pathway prevents CD4+ T cell-mediated colitis in a Th17-independent manner. *Int. Immunol.* **19**, 1431–1440 (2007).
21. Izcue, A. *et al.* Interleukin-23 restrains regulatory T cell activity to drive T cell-dependent colitis. *Immunity* **28**, 559–570 (2008).
22. Leppkes, M. *et al.* RORγ-expressing Th17 cells induce murine chronic intestinal inflammation via redundant effects of IL-17A and IL-17F. *Gastroenterology* **136**, 257–267 (2009).
23. O'Connor, W. Jr. *et al.* A protective function for interleukin 17A in T cell-mediated intestinal inflammation. *Nat. Immunol.* **10**, 603–609 (2009).
24. Simpson, S.J. *et al.* T cell-mediated pathology in two models of experimental colitis depends predominantly on the interleukin 12/Signal transducer and activator of transcription (Stat)-4 pathway, but is not conditional on interferon γ expression by T cells. *J Exp. Med.* **187**, 1225–1234 (1998).
25. Neurath, M.F. *et al.* The transcription factor T-bet regulates mucosal T cell activation in experimental colitis and Crohn's disease. *J. Exp. Med.* **195**, 1129–1143 (2002).
26. Durant, L. *et al.* Diverse targets of the transcription factor STAT3 contribute to T cell pathogenicity and homeostasis. *Immunity* **32**, 605–615 (2010).
27. Feng, T. *et al.* Th17 cells induce colitis and promote Th1 cell responses through IL-17 induction of innate IL-12 and IL-23 production. *J. Immunol.* **186**, 6313–6318 (2011).
28. Wei, G. *et al.* Global mapping of H3K4me3 and H3K27me3 reveals specificity and plasticity in lineage fate determination of differentiating CD4+ T cells. *Immunity* **30**, 155–167 (2009).
29. Bending, D. *et al.* Epigenetic changes at *Il12rb2* and *Tbx21* in relation to plasticity behavior of Th17 cells. *J. Immunol.* **186**, 3373–3382 (2011).
30. Mukasa, R. *et al.* Epigenetic instability of cytokine and transcription factor gene loci underlies plasticity of the T helper 17 cell lineage. *Immunity* **32**, 616–627 (2010).
31. Lexberg, M.H. *et al.* Th memory for interleukin-17 expression is stable *in vivo*. *Eur. J. Immunol.* **38**, 2654–2664 (2008).
32. Lexberg, M.H. *et al.* IFN-g and IL-12 synergize to convert *in vivo* generated Th17 into Th1/Th17 cells. *Eur. J. Immunol.* **40**, 3017–3027 (2010).
33. Stevens, E.A., Mezrich, J.D. & Bradfield, C.A. The aryl hydrocarbon receptor: a perspective on potential roles in the immune system. *Immunology* **127**, 299–311 (2009).
34. Lee, Y.K. *et al.* Late developmental plasticity in the T helper 17 lineage. *Immunity* **30**, 92–107 (2009).
35. Powrie, F., Correa-Oliveira, R., Mauze, S. & Coffman, R.L. Regulatory interactions between CD45RB^high and CD45RB^low CD4+ T cells are important for the balance between protective and pathogenic cell-mediated immunity. *J. Exp. Med.* **179**, 589–600 (1994).
36. Powrie, F. *et al.* Inhibition of Th1 responses prevents inflammatory bowel disease in *scid* mice reconstituted with CD45RB^hi CD4+ T cells. *Immunity* **1**, 553–562 (1994).
37. Berg, D.J. *et al.* Enterocolitis and colon cancer in interleukin-10-deficient mice are associated with aberrant cytokine production and CD4+ TH1-like responses. *J. Clin. Invest.* **98**, 1010–1020 (1996).
38. El-Behi, M. *et al.* The encephalitogenicity of TH17 cells is dependent on IL-1- and IL-23-induced production of the cytokine GM-CSF. *Nat. Immunol* **12**, 568–575 (2011).
39. Codarri, L. *et al.* RORγt drives production of the cytokine GM-CSF in helper T cells, which is essential for the effector phase of autoimmune neuroinflammation. *Nat. Immunol.* **12**, 560–567 (2011).
40. Hueber, W. *et al.* Inhibition of IL-17A by secukinumab is inefffective for Crohn's disease (CD). *J. Crohn's Colitis* **5**, S7 (2011).
41. Kühn, R., Löhler, J., Rennick, D., Rajewsky, K. & Müller, W. Interleukin-10-deficient mice develop chronic enterocolitis. *Cell* **75**, 263–274 (1993).
42. Ward, J.M., Anver, M.R., Haines, D.C. & Benveniste, R.E. Chronic active hepatitis in mice caused by *Helicobacter hepaticus. Am. J. Pathol.* **145**, 959–968 (1994).
43. Ge, Z., White, D.A., Whary, M.T. & Fox, J.G. Fluorogenic PCR-based quantitative detection of a murine pathogen *Helicobacter hepaticus. J. Clin. Microbiol.* **39**, 2598–2602 (2001).
44. Maloy, K.J. *et al.* CD4+CD25+ T_R cells suppress innate immune pathology through cytokine-dependent mechanisms. *J. Exp. Med.* **197**, 111–119 (2003).